

## Chemical and Isotopic Geothermometers to Estimate Geothermal Reservoir Temperature and Vapor Fraction

Mahendra P. Verma

Geotermia, Instituto de Investigaciones Eléctricas, Reforma 113, Col. Palmira, Cuernavaca, Mor., C.P. 62490, México  
mahendra@iie.org.mx

**Keywords:** Geothermometry, Los Azufres, state function, silica solubility, stable isotope exchange, thermodynamics.

### ABSTRACT

According to thermodynamics, the equilibrium constant of a chemical or isotopic fractionation reaction is a state function and in general is a function of two state variables (e.g. temperature and pressure). Depending on the type of species involved in the reaction, it can be used as geothermometer and/or geobarometer. Using these thermodynamic concepts, the chemical and isotopic geothermometers: *silica solubility, cation-exchange, methane breakdown, and oxygen-18 in dissolved sulfate and water* are revised. The cation exchange geothermometer is a violation of laws of chemistry and thermodynamics, and is not used in this study. The Los Azufres reservoir temperature is in the range 190-310°C with an uncertainty of  $\pm 20^\circ\text{C}$  and the vapor fraction is 13-85% with uncertainty of  $\pm 2\%$ . This suggests the existence of liquid-vapor phase segregation within the reservoir.

### 1. INTRODUCTION

Geochemical study of geothermal system contemplates an understanding of mechanisms of physical-chemical processes responsible for its origin and evolution. The chemical compositions of fluids (separated vapor and water), collected from fumaroles, hot springs and drilled wells at the Earth surface are determined in the laboratory (Verma, 2002a). In the geothermal industry, the estimation of deep reservoir temperature is essential for proper mining and utilization of geothermal heat. Consequently, various geothermometers have been proposed: *silica solubility geothermometers, cation exchange geothermometers, gas geothermometers* and *stable isotope geothermometers*. This article describes the chemical and isotopic geothermometers from the thermodynamic point of view and presents their application in determining the reservoir characteristics of Los Azufres geothermal system, Mexico.

### 2. AN OVERVIEW ON THERMODYNAMICS

Human being has invented various types of machines to convert different types of energies into work for making life more comfortable. In these energy conversion processes, the mankind has learnt the existence of some rules of nature which are known as the laws of thermodynamics: *0<sup>th</sup> law: definition of temperature, 1<sup>st</sup> law: conservation of energy and 2<sup>nd</sup> law: direction of spontaneous process*. Thermodynamic laws were well established by the end of nineteenth century and various excellent textbooks were written in the twentieth century to describe these laws from different points of view (Verma, 2006). The intensive parameters (i.e. molar quantity in the case of extensive parameters) are here used to avoid the consideration of mass factor.

1. Temperature (T), pressure (P), volume (V), internal energy (U), enthalpy (H), entropy (S), Gibbs free energy (G), Helmholtz energy (A), conductivity, solubility, equilibrium constant of a chemical reaction, etc. are state functions.
2. Any two state functions are sufficient and necessary to define completely a pure homogeneous system in a phase.
3. The variation of a state function between two points is independent of trajectory (path) and the past history of the substance.
4. If Z is a dependent state function of two state variables X and Y, it should fulfill the following relations of a mathematical exact function.

$$\frac{\partial^2 Z}{\partial Y \partial X} = \frac{\partial^2 Z}{\partial X \partial Y} \quad (1)$$

$$\left(\frac{\partial Z}{\partial X}\right)_Y \left(\frac{\partial X}{\partial Y}\right)_Z \left(\frac{\partial Y}{\partial Z}\right)_X = -1 \quad (2)$$

If one independent variable (say Y) is constant, the equation 2 reduces to

$$\left(\frac{\partial X}{\partial Z}\right) \left(\frac{\partial Z}{\partial X}\right) = 1 \quad (3)$$

These properties of exact functions (i.e. equations 1 to 3) show clearly that there cannot be maximum-minimum (i.e. multi-valued functions) in the behavior state functions. If the same value of Z exists for two values of X (say  $x_1$  and  $x_2$ ) at constant Y, there should be at least one minimum or maximum in the behavior of Z or the same value of Z for any value of X between  $x_1$  and  $x_2$ . Figure 1 shows various possible behaviors of Z. At the minimum or maximum (say at the maximum point m), one can write  $\Delta X = \pm ve$ ,  $\Delta Z = 0$ ,  $(\partial Z / \partial X) = 0$  and  $(\partial X / \partial Z) = \infty$ . Thus  $(\partial Z / \partial X)(\partial X / \partial Z) = 0 \times \infty$ . (i.e. indeterminate, but not equal to 1).

Figure 2 presents the impermissible behavior of state function Z, considering X as independent and Y as constant. Figure 2a shows multiple-values of Z or X. Similarly, the crossing of tendencies implies multiple values (Figure 2b). In Figure 2c there is a point of inflection in the tendencies between X and Z while Y is constant, which indicates a discontinuity in the derivative of X with Z and vice-versa. Additionally, there should not be any crossing on either side of the point of inflection and the plots for different values of

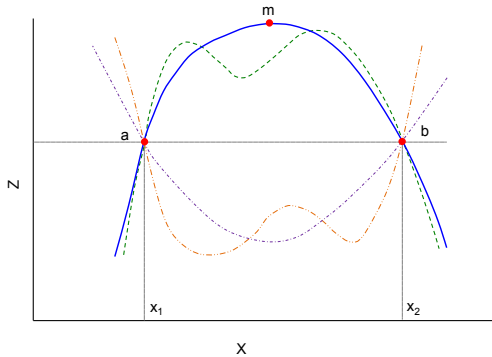


**Figure 1: Hypothetical behaviors of a state function Z as a function of independent state variable X, if there is same value of Z for two values of X at points a and b (Verma, 2006).**

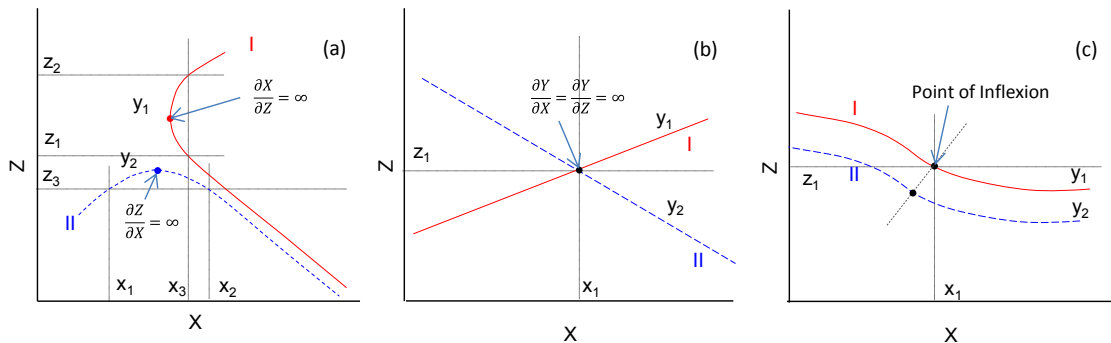


**Figure 2: Impermissible behaviors of a state function in a pure phase: (a) multiple values, (b) crossing of tendency and (c) point of inflection (Verma, 2006).**

Y should be approximately parallel (i.e. independent of Y). Otherwise, if these tendencies are re-plotted between X (or Z) and Y at constant Z (or X), there will be a crossing in the behavior of state functions X (or Z) and Y.

Thermodynamics does not impose any restriction on the behavior of a state function (say Z) with respect to independent state variables (say X and Y) for a system. However, if we know the behavior of X with Y and the behavior of Z with X (or Y), we can predict the behavior of Z with Y (or X) according to equation 2. For example, in the case of an ideal gas system at constant V, T increases with increasing P. If V increases with T, it should decrease with P. Similarly, on considering T and P as independent variables, V is uniquely defined. That is true in case of ideal gas.

### 3. GEOTHERMOMETRY

In the geothermal industry, the estimation of deep reservoir temperature is essential for proper mining and utilization of geothermal heat. Figure 3 shows the conceptual diagram of geothermal system with n-separators (Verma, 2012a). The last separator in the separation cycle (i.e. the weir box) is considered as the first separator. For geochemical calculations with the propagation of analytical uncertainty, the liquid and condensed vapor samples are generally collected at the first and second separators, respectively. The first separator pressure may be different from the atmospheric pressure. If the separation pressure is higher than the atmospheric pressure, the separated liquid is passed through a cooling coil attached to the separator in order to collect the sample. Using the geothermometers and mass, energy and alkalinity conservation, the chemical concentrations are converted to the reservoir conditions to predict the state of water-rock interaction and reservoir processes like boiling, condensation, mixing with other fluids, mineral dissolution-precipitation, etc. Various geothermometers have been proposed: *silica solubility geothermometers*, *cation exchange geothermometers*, *gas geothermometers* and *stable isotope geothermometers*. The derivation of these geothermometers from the thermodynamic point of view including the propagation of analytical uncertainty (error) in each algorithm is presented here.

#### 3.1 Silica Geothermometry

The development of silica geothermometry commenced with the pioneer work of White et al. (1956) as the silica concentration in hot springs at Steamboat, Nevada was very close to the experimental solubility of amorphous silica. Silica exists naturally in many stable phases including quartz, chalcedony, tridymite, cristobalite, coesite, stishovite and amorphous silica. The dissolution-precipitation equilibration of such multi-phase minerals depends upon the solution-mineral contact time, and it requires an understanding of mineral solubility kinetics (Stumm and Morgan, 1981).

Numerous geothermometers have been proposed on the basis of solubility data along the saturation curve of quartz, chalcedony, Cristobalite and amorphous silica (Fournier, 1977a; Fournier and Potter, 1982; Verma and Santoyo, 1997; Gunnarsson and Arnorsson, 2000; Verma, 2002a, 2003a; Verma and Betzler, 2013). We will focus here on the extreme phases (i.e. quartz and

amorphous) silica solubility geothermometers, which have applicability to the geothermal reservoir and natural manifestation fluids, respectively.

The silica dissolution results in the formation of silicic acid according to the following reaction

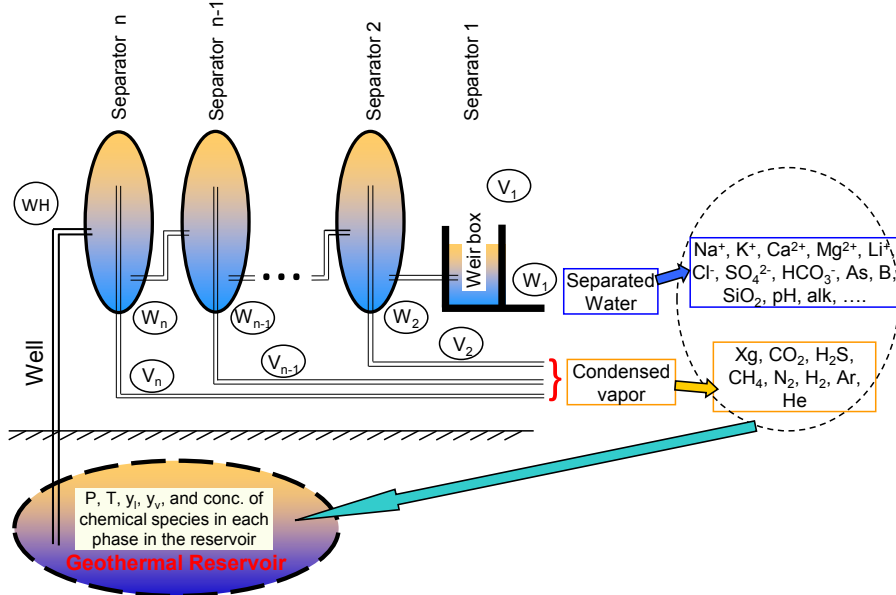


**Figure 3:** Schematic diagram of a geothermal system to illustrate the extraction of geothermal fluid from a well and its separation into vapor and liquid in  $n$ -separators. The last separator in the separation cycle (i.e. the weir box) is considered as the first separator (after Verma, 2012a). The first step of the geochemical calculation procedure is the reconstruction the reservoir fluid characteristics (i.e. pressure (P), temperature (T), fraction of liquid ( $y_l$ ) and vapor ( $y_v$ ), and concentration of chemical and isotopic species in the liquid and vapor phases).



The equilibrium constant for chemical reaction (equation 4) is expressed as

$$K_{SiO_2} = \exp\left(\frac{-\Delta G_F^{T,P}}{RT}\right) = \frac{a_{H_2SiO_4}}{a_{SiO_2} \cdot a_{H_2O}} \cong a_{H_2SiO_4} \cong [H_2SiO_4] \quad (5)$$

where  $\Delta G_F^{T,P}$  is the difference in the Gibbs free energy of formation of the participating species (i.e. products minus reactants) at any temperature ( $T$ ) and pressure ( $P$ ), subscript  $F$  stands for formation,  $R$  is the gas constant, and ' $a$ ' is the activity of respective species. If we assume water and solid silica as pure phases, the equilibrium constant is equal to the activity of  $H_2SiO_4$ . Further, on assuming the activity coefficient for  $H_2SiO_4$  as unity, the equilibrium constant ( $K_{SiO_2}$ ) reduces to the molal concentration of  $H_2SiO_4$ . There exist various dissociated species of silica acid in solution and their concentration depends on the solution pH. In the case of natural aqueous solutions the undissociated form (i.e.  $H_2SiO_4$ ) is the dominating species, therefore the total dissolved silicic species concentration ( $SiO_{2(aq)}$ ) is equal to  $[H_2SiO_4]$  and the equation 5 may be written as

$$\log SiO_{2(aq)} = \frac{1}{2.303} \left( \frac{-\Delta G_F^{T,P}}{RT} \right) = \frac{1}{2.303} \left( \frac{-\Delta H_F^{T,P}}{RT} \right) + \frac{1}{2.303} \left( \frac{\Delta S^{T,P}}{R} \right) \quad (6)$$

At lower temperatures, the values of Gibbs free energy ( $\Delta G_F^{T,P}$ ), or enthalpy ( $\Delta H_F^{T,P}$ ) and entropy ( $\Delta S^{T,P}$ ) are constant for the first order approximation and the variation of  $\log K$  with  $1/T$  is a straight line; however, there could be small deviation from the linear behavior of silica solubility at high temperature and pressure as  $\Delta G_F^{T,P}$  or  $\Delta H_F^{T,P}$  and  $\Delta S^{T,P}$  are function of  $T$  and  $P$ . This approximation is only valid if the solid and liquid species are involved in the chemical reaction. In case of gaseous species the equilibrium constant of chemical reaction is always a function of  $T$  and  $P$ .

Along the liquid-vapor saturation curve,  $P$  is defined by  $T$  and vice-versa; however,  $P$  (or  $T$ ) is not constant. Therefore, Verma (2003a) suggested the fitting the quartz solubility data in a quadratic equation of  $1/T$  and  $P$  of the following form

$$\log SiO_2(ppm) = a + b \frac{1}{T} \ln K + c P(MPa) + d \frac{1}{T^2} + e \frac{P}{T} + f P^2 \quad (7)$$

The equation 1 (i.e. the first constraint of exact function) was internally fulfilled in the above polynomial. However, Verma and Betzler (2013) improved the polynomial fitting with implementing the second constraint (i.e. equation 2) of exact function, which is rewritten as

$$\left( \frac{\partial P}{\partial T} \right)_{CS} \left( \frac{\partial T}{\partial CS} \right)_P \left( \frac{\partial CS}{\partial P} \right)_T = -1, \text{ where } CS = \log SiO_2(ppm) \quad (8)$$

The values of  $\left(\frac{\partial P}{\partial T}\right)_{CS}$  at a given T and P are obtained from steam tables. With differentiating equation 7 with respect to T and P, we can calculate the values of  $\left(\frac{\partial T}{\partial CS}\right)_P$  and  $\left(\frac{\partial CS}{\partial P}\right)_T$ . On substituting them in equation 8, we get

$$-1/T^2 b + \left(\frac{\partial P}{\partial T}\right)_{CS} c - 2/T^3 d + \left(\left(\frac{\partial P}{\partial T}\right)_{CS} \frac{1}{T} - \frac{P}{T^2}\right) e + 2P \left(\frac{\partial P}{\partial T}\right)_{CS} f = 0 \quad (9)$$

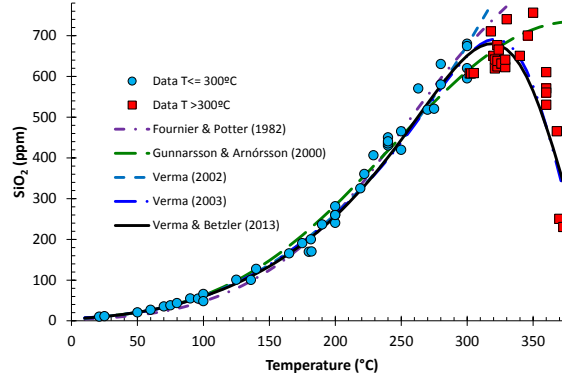


**Figure 4(a): Quartz solubility experimental data along the liquid-vapor saturation curve together with the plot of various polynomials for quartz solubility given in Table 1.**

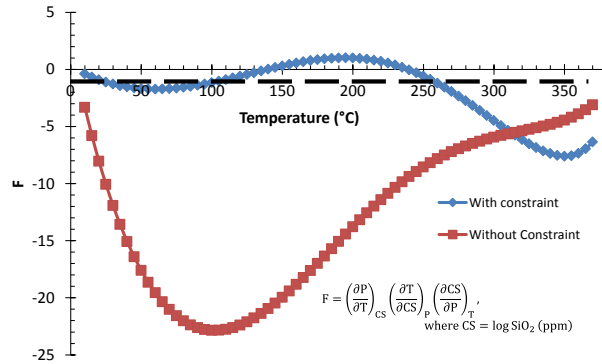


**Figure 4(b): Plot of F with temperature for the quadratic polynomials of quartz solubility data, derived without and with implementing the constraints (i.e. equations 1 and 2) of exact function. The line (F=-1) is shown with dashed line.**

**Table 1: Quartz and amorphous silica solubility regression equations**

Equation*	Type
	Quartz
$T = 230.952 + 0.28831 SiO_2 - 3.6686 \times 10^{-4} SiO_2^2 + 3.1665 \times 10^{-7} SiO_2^3 + 77.03 \log SiO_2$	Polynomial of SiO <sub>2</sub> (Fournier & Potter, 1982)
$\log SiO_2 = -29.41 + 197.47/T - 5.851 \times 10^{-6} T^2 + 12.245 \log T$	Polynomial of T (Gunnarsson & Arnórsson, 2000)
$\log SiO_2 = -1117.34(\pm 13.05)/T + 4.78(\pm 0.03)$	Linear of 1/T (Verma, 2002a)
$\log SiO_2 = 6.1393 - 2031.11/T - 0.33262 P - 1.5305 \times 10^5/T^2 - 189.44 P/T - 3.6102 \times 10^{-3} P^2$	Quadratic of 1/T and P (refitted after Verma 2003a)
$\log SiO_2 = 4.6970 - 1080.13/T + 0.06808 P - 3295.02/T^2 - 27.44 P/T - 2.200 \times 10^{-3} P^2$	Quadratic of 1/T and P with exact function constraint $\left(\frac{\partial P}{\partial T}\right)_S \left(\frac{\partial T}{\partial S}\right)_P \left(\frac{\partial S}{\partial P}\right)_T = -1$ , where $S = \log SiO_2$ (Verma & Betzler, 2013).
	Amorphous silica
$\log SiO_2 = -731/T + 4.52$	Linear of 1/T (Fournier 1977a)
$\log SiO_2 = 3.7983 - 225.10/T - 0.1815 P - 8.6689 \times 10^4/T^2 + 92.943 P/T + 3.874 \times 10^{-3} P^2$	Quadratic of 1/T and P without exact function constraint (Verma, 2014)
$\log SiO_2 = 4.0930 - 409.25/T + 0.0169 P - 5.7666 \times 10^4/T^2 - 9.192 P/T + 5.539 \times 10^{-4} P^2$	Quadratic of 1/T and P with exact function constraint (Verma, 2014)

\*Temperature (T) in K, Pressure (P) in MPa, and Silica (SiO<sub>2</sub>) in ppm.

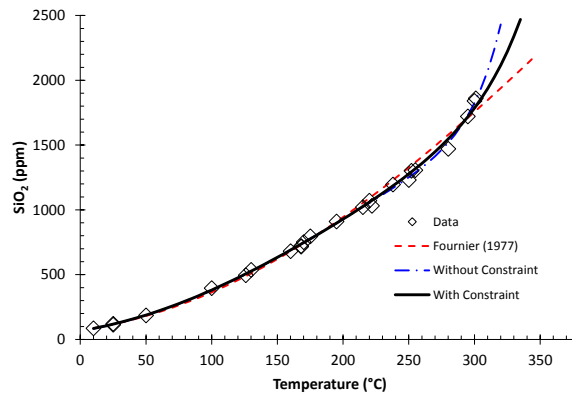


**Figure 5(a): Experimental data of amorphous silica solubility along the liquid-vapor saturation curve together with the plot of various polynomials for amorphous silica given in Table 1.**

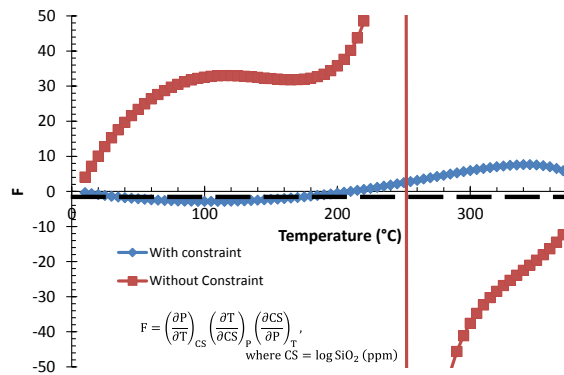


**Figure 5(b): Plot of F with temperature for the quadratic polynomials of amorphous solubility data, derived without and with implementing the constraints (i.e. equations 1 and 2) of exact function. The line ( $F=-1$ ) is shown with dashed line.**

So, the equation 9 for all the values of measured silica concentration at given  $T$  and  $P$  must be included in the least square fitting of solubility polynomial (equation 7).

### 3.1.1 Quartz Solubility Data

In a geothermal reservoir the fluid residence time is sufficiently large to get the quartz solubility equilibrium. Verma (2000) compiled the experimental quartz solubility data along the saturation curve. These experimental quartz solubility data have been fitted to five different types of equations (Table 1): (i) *temperature as a polynomial of  $SiO_2$  including logarithmic terms* (Fournier and Potter, 1982), (ii) *a polynomial of absolute temperature including logarithmic terms* (Gunnarsson and Arnórsson, 2000) (iii) *a linear equation relating  $\log SiO_2$  to the inverse of absolute temperature* (Verma, 2002a), (iv) *a quadratic equation of  $1/T$  and  $P$*  (Verma, 2003) and (v) *a quadratic equation of  $1/T$  and  $P$  with the exact function constraint* (Verma and Betzler, 2013).

The equations together with the experimental quartz solubility data are plotted in Figure 4a. The data are divided in two groups:  $T \leq 300^\circ C$  and  $T > 300^\circ C$ . It can be observed that the earlier equations (i.e. Fournier and Potter, 1982; Gunnarsson and Arnórsson, 2000; Verma 2002a) do not fit the experimental data above  $320^\circ C$ . But both the quadratic polynomial equations, without (Verma, 2003a) and with constraints (Verma and Betzler, 2013) of exact function (Table 1) fit well all the quartz solubility data (Figure 4a).

Figure 4b shows the behavior of  $F = \left( \frac{\partial P}{\partial T} \right)_{CS} \left( \frac{\partial T}{\partial CS} \right)_P \left( \frac{\partial CS}{\partial P} \right)_T$ , where  $CS = \log SiO_2$  (ppm) for the quadratic polynomial equations, without and with the constraints of exact function with temperature along the liquid-vapor saturation curve. According to the discussion presented above, it should be a straight line (i.e.  $F = -1$ ). It can be observed that the behavior of quadratic polynomial equation with the constraints of exact function fluctuates along the straight line. In other words, the implementation of the constraints of exact function is necessary for the curve fitting of thermodynamic data, although the development of quartz solubility geothermometers based on any of the polynomial equations will provide the geothermal reservoir temperature within the analytical uncertainty of silica concentration measurement as all the equations (Table 1) are very close together up to  $300^\circ C$ .

### 3.1.2 Amorphous Silica Solubility Data

The amorphous silica solubility data together with the polynomial equations (Table 1) are plotted in Figure 5a. The data are only up to  $300^\circ C$ . Fournier (1977b) presented an extrapolation of amorphous silica solubility data based on the quartz solubility data. Verma (2013) demonstrated that the measurement of heat capacity of water at higher temperature has experimental difficulty due to

the existence of water vapor in the experimental setup. This is also true even for the silica solubility measurements. Thus the decrease in quartz solubility after 330°C may be an artifact of experimental difficulties, which is needed to be verified with new experimental silica solubility data.

Figure 5b shows the temperature behavior of  $F \left( = \left( \frac{\partial P}{\partial T} \right)_{CS} \left( \frac{\partial T}{\partial CS} \right)_P \left( \frac{\partial CS}{\partial P} \right)_T \right)$ , where  $CS = \log SiO_2 (ppm)$  for the quadratic polynomial equations for amorphous silica solubility data, without and with the constraints of exact function. The behavior of quadratic polynomial equation with the constraints of exact function fluctuates along the straight line (i.e.  $F = -1$ ). Again, the implementation of the constraints of exact function is necessary for the curve fitting of thermodynamic data. However, the development of amorphous silica solubility geothermometers based on any of the polynomial equations (Table 1) will provide the same temperature up to 300°C.

### 3.1.3 Algorithm for Silica Geothermometer

Verma (2008) presented an algorithm based on the conservation of enthalpy and silica to estimate temperature and vapor fraction in a geothermal reservoir. Verma (2012a) improved the algorithm with the propagation of analytical uncertainty in the measured parameters. The geothermal reservoir conditions are generally along the liquid-vapor saturation and there may be any proportion of vapor from 0 to 100% in the reservoir. Silica dissolves only in the liquid phase. In the development of silica geothermometry, the following assumptions are made here (Henley et al., 1984): (a) There is single feed zone to the geothermal well and no phase segregation in the reservoir and in the well. In other word there is homogeneous flow in the well, (b) The total discharge fluid from a well represents both the liquid and vapor phases in the reservoir i.e. the total discharge enthalpy is the reservoir enthalpy and (c) There is no adiabatic condensation.

The first is the calculation of total discharge concentration.

According to the conservation of enthalpy, the vapor fraction at the  $i^{\text{th}}$  separator is expressed as

$$y_{(i)} = \frac{H_{l(i+1)} - H_{l(i)}}{H_{v(i)} - H_{l(i)}}, \quad i = 1, 2, \dots \text{to} \dots nSep - 1 \quad (10)$$

where  $nSep$  is the total number of separators (Figure 3).  $H$  is enthalpy and subscripts  $l$  and  $v$  represent the liquid and vapor phases, respectively. The vapor fraction at the  $nSep$ - separator is calculated as

$$y_{(nSep)} = \frac{H_{res} - H_{l(nSep)}}{H_{v(nSep)} - H_{l(nSep)}} \quad (11)$$

where  $H_{res}$  is the measured reservoir enthalpy. The concentration of silica at separator 1 is the measured concentration of water sample. Thus the concentration at other separators is calculated as

$$SiO_{2(i+1)} = \{1 - y_{(i)}\} SiO_{2(i)}, \quad i = 1, 2, \dots \text{to} \dots nSep - 1 \quad (12)$$

The total discharged concentration is

$$SiO_{2,TD} = \{1 - y_{(nSep)}\} SiO_{2(nSep)} \quad (13)$$

Similarly, the measured uncertainty of silica in water samples is the uncertainty at the first separator. The uncertainty of measured silica concentration is propagated according to the following equation

$$SiO_2 Err_{(i+1)} = \{1 - y_{(i)}\} SiO_2 Err_{(i)}, \quad i = 1, 2, \dots \text{to} \dots nSep - 1 \quad (14)$$

The uncertainty of total discharged concentration is

$$SiO_2 TDErr = \{1 - y_{(nSep)}\} SiO_2 Err_{(nSep)} \quad (15)$$

The second step is the geothermal reservoir temperature and vapor fraction with uncertainty propagation. The equation for the conservation of silica in the geothermal reservoir is written as

$$SiO_{2,TD} = \{1 - y_{res}\} SiO_{2,l} \quad (16)$$

where  $SiO_{2,TD}$  is the total discharge concentration of silica,  $y_{res}$  is the reservoir vapor fraction and  $SiO_{2,l}$  is the silica concentration in liquid phase in the reservoir. From equation 16, the fraction of vapor in the reservoir as

$$y_{res} = 1 - \frac{SiO_{2,TD}}{SiO_{2,l}} \quad (17)$$

Let the temperature in the reservoir be  $T$ . The value of  $T$  (and the corresponding saturated pressure ( $P$ ) for the quadratic regression equation) is substituted in the regression equations given in Table 1 to calculate the silica concentration of liquid phase in the reservoir. This silica concentration ( $SiO_{2,poly}$ ) is substituted for  $SiO_{2,l}$  in equation 17 to calculate  $y_{res}$ . The value of  $y_{res}$  together with the values of  $H_l$  and  $H_v$  at  $T$  are used to calculate the reservoir enthalpy ( $H_{res}$ ) from equation 1.  $H_{res}$  must be equal to the measured reservoir enthalpy ( $H_R$ ), if  $T$  is equal to the reservoir temperature. Thus the equation 17 and the conservation of enthalpy ( $H_{res} = (1 - y_{res})H_l + y_{res}H_v$ ) are solved for temperature and vapor fraction.

Verma (2012a) included this algorithm in the computer program, QrtzGeotherm for the propagation of analytical uncertainty in the calculation of geothermal reservoir parameters. The program is modified to SilicaGeotherm with including amorphous silica geothermometry and the solubility polynomials with the constraints of exact function.

The independent variables are reservoir enthalpy ( $H_R$ ) and total discharge concentration of  $SiO_2$  ( $SiO_{2,TD}$ ), whereas the dependent variables are reservoir temperature ( $T_{Res}$ ) and vapor fraction ( $y_{Res}$ ). Fortunately, the number of both independent and dependent variables is same, but the algorithm is valid for any number of independent and dependent variables.

### 3.2 Cation Exchange Geothermometry

S.P. Verma (2002) compiled the equations of various types of cation exchange geothermometers, which are empirical relations used to estimate deep geothermal reservoir temperature on the basis of the proportion of cation concentrations (e.g.  $Na^+/K^+$ ) in geothermal fluid. Most commonly used cation geothermometers based on the concentration of  $Na^+$ ,  $K^+$ ,  $Ca^{2+}$  and/or  $Mg^{2+}$  are from Fournier and Truesdell (1973) and others. Verma and Santoyo (1997) applied a statistical data treatment method and the theory of error propagation in improving the  $Na^+/K^+$  geothermometer equation. Arnónsson (2000) presents a thermodynamic calibration for the  $Na^+/K^+$  geothermometer equation.

A cation-exchange reaction between  $Na^+$  and  $K^+$  is in general written as following



where X represents an anion and z denotes the stoichiometric coefficient. The equilibrium constant of this reaction is given by

$$K_{eq} = \exp\left(-\frac{\Delta G_F^{T,P}}{RT}\right) = \frac{(a_{K^+})^z(a_{Na_zK_{1-z}X})}{(a_{Na^+})^z(a_{Na_{1-z}K_zX})} \quad (19)$$

The activity coefficient is considered to unity in dilute solutions. Similarly, the activity of solid phases is also considered as unity in developing the geothermometers. The equilibrium constant (equation 20) is reduced to

$$K_{eq} = \left(\frac{[K^+]}{[Na^+]} \right)^z \quad (20)$$

Thus the proportion of  $Na^+/K^+$  in geothermal fluids is a function of T and P. The pressure effect is considered relatively less under the geothermal reservoir conditions.

Verma(2012a) and Verma and Betzler (2013) analyzed the above treatment for the development of cation exchange geothermometers on the basis of the laws of chemistry and chemical thermodynamics:

- *Unidirectionality:* There are some materials which have affinity to capture some cation (say  $Na^+$ ) and liberate other cation (say  $K^+$ ) under certain environmental conditions. These types of reactions are unidirectional for the given environment. Writing a chemical reaction like equation 19 with “=” sign means that the reaction is in equilibrium (i.e. some reactants form products and the equal amount products form reactants). In other words there is equilibrium between reactants ( $Na^+$ ,  $Na_{1-z}K_zX$ ) and products ( $K^+$ ,  $Na_zK_{1-z}X$ ). Clearly, this is not true in case of exchange reaction.
- *Activity Coefficient of Impure Mineral:* The mixed-minerals like  $Na_{1-z}K_zX$  are not pure phase, so their activity cannot be considered as unity.
- *Imbalanced Reaction:* On substituting  $z = 0.5$ , the equation 19 reduces to



- *Inexistence of Free Ions:* There is need is to know the structural formula of the molecule or species. According to equation 22 the reactants ( $Na^+$ ,  $KX$ ) form products ( $K^+$ ,  $NaX$ ). We cannot have free ions. It means that equation 22 (or 19) is a partial chemical reaction. Thus there is need to understand first the full chemical reaction instead of developing a geothermometer on the basis of partial chemical reaction.
- *Electro-neutrality of Solution:* According to equation 22 (or 19) there are  $Na^+$  and  $K^+$  in the solution and both have positive charge. A solution should be electrically neutral. It means that the concentrations of  $Na^+$  and  $K^+$  must be controlled by some anions in the solution. We have to know the effect of controlling anions on the equilibrium constant of the “cation exchange” reaction.
- *Arbitrary Temperature Value:* Fournier (1989) simplified the equations for various cation-exchange geothermometers to the  $Na^+/K^+$  geothermometer. Then he plotted  $\log (Na^+/K^+)$  versus  $1000/T$  for base exchange between albite and adularia, albite and microlite and  $Na^+$ - and  $K^+$ -montorillonites together with the values of  $\log (Na^+/K^+)$  for the empirical equations (Figure 6). There is a wide range of values for  $\log (Na^+/K^+)$  at a given temperature and vice versa. For example, at temperature 100°C,  $\log (Na^+/K^+)$  varies in the range 0.95 to 2.25 for different equations. Similarly, for  $\log (Na^+/K^+)=1.00$ , the temperature range is 90 to 410°C. Thus one can get a wide range of temperature values using different geothermometer equations for a given ratio of  $Na^+/K^+$ .

Thus the *cation exchange geothermometry* is contradictory to the *laws of chemistry and chemical thermodynamics* and must be abandoned, if we are unable to justify any of the above mentioned points.

### 3.3 Gas Geothermometry

The gas geothermometers for the  $H_2O-CO_2-H_2S-NH_3-H_2-N_2CH_4$  system have been proposed by Giggenbach (1980) and others. These geothermometers are useful in case of vapor-dominated (or vapor producing) geothermal systems. We will discuss the

approach of Giggenbach (1980) with the thermodynamic point of view. There are generally two phases, liquid and vapor in a geothermal reservoir. The methane breakdown reaction for the vapor phase may be written as

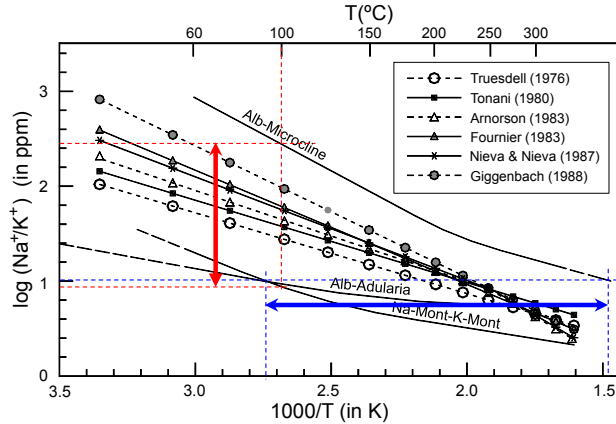


**Figure 6: Variation of  $\log(Na^+/K^+)$  as a function of  $1000/T$  for the theoretical curves for low albite-microcline, low albite-adularia, and Na-montmorillonite-K-montmorillonite together with equation of various  $Na^+/K^+$  geothermometers (modified after Fournier, 1989).**

Considering the fugacity coefficients as unity, the equilibrium constant of the reaction 23 in terms of partial pressure ( $P_i$ ) of respective species may be written

$$K_C = \frac{P_{CO_2} P_{H_2}^4}{P_{CH_4} P_{H_2O}^2} \quad (23)$$

By substituting the relationship

$$P_i = x_{v,i} P_t \quad (24)$$

where  $x_{v,i}$  represents the mole fraction of the gas  $i$  in the vapor phase at a total pressure  $P_t$ , equation 24 changes to

$$K_C = \frac{x_{v,CO_2} x_{v,H_2}^4 P_t^4}{x_{v,CH_4} P_{H_2O}^2} \quad (25)$$

The distribution coefficient of gaseous species  $i$  between vapor and liquid is defined as

$$B_i = \frac{x_{v,i}}{x_{l,i}} = \frac{\left(\frac{n_i}{n_{H_2O} + \sum n_i}\right)_v}{\left(\frac{n_i}{n_{H_2O} + \sum n_i}\right)_l} \cong \frac{\left(\frac{n_i}{n_{H_2O}}\right)_v}{\left(\frac{n_i}{n_{H_2O}}\right)_l} \quad (26)$$

On substituting the values of  $x_{v,i}$  from equation 27 in equation 26, we get

$$K_C = \frac{x_{l,CO_2} B_{CO_2} x_{l,H_2}^4 B_{H_2}^4 P_t^4}{x_{l,CH_4} B_{CH_4} P_{H_2O}^2} \quad (27)$$

The effect of vapor gain or loss on the liquid phase concentration in terms of the total well discharge concentration is expressed as

$$x_{l,i} = \frac{x_{d,i}}{(1 - y + yB_i)^{\pm 1}} = \frac{x_{d,i}}{D_i^{\pm 1}} \quad (28)$$

The values of  $K_C$  and  $P_{H_2O}$  as function of  $T$  (in K) are the following

$$\log K_C = 10.76 - 9323/T \quad (30)$$

$$\log P_{H_2O} = 5.51 - 2048/T \quad (31)$$

Similarly, the values of  $B$  for  $CH_4$ ,  $H_2$  and  $CO_2$  are function of  $T$  (Giggenbach, 1980). However, the following important points are lacking in this derivation of gas geothermometer:

- The equilibrium constant of a chemical reaction which involves gaseous species must be a function of T and P. Giggenbach (1980) did not describe the derivation of  $K_C$ ,  $P_{H_2O}$  and coefficient of distribution (B) of gaseous species as function of T.
- Verma (2002b) showed that the concentration of  $CO_2$  in the total discharge of a well was also function of geothermal reservoir liquid pH.
- Giggenbach et al. (2001) showed that the sampling procedure of gaseous species in geothermal fluids was incorrect. Thus it is not justified to obtain valid results on the characteristics of geothermal reservoir form these gaseous species data.

Thus the gas geothermometry concepts need to be improved with the basic knowledge of chemistry and chemical thermodynamics. Similarly, the gas sampling techniques are very primitives.

### 3.4 Stable Isotope Geothermometry

An isotopic exchange reaction (Urey, 1947) may be written as

$$a A_1 + b B_2 = a A_2 + b B_1 \quad (32)$$

where A and B are molecules which have some one element as a common constituent and the subscripts 1 and 2 indicate that the molecule contains only the light or the heavy isotope, respectively. The equilibrium constant of the isotopic exchange reaction is defined as

$$K = \frac{\left(\frac{Q'_A}{Q'_B}\right)^a}{\left(\frac{Q'_B}{Q'_A}\right)^b} \quad (33)$$

where the  $Q'$ 's are the partition functions of the molecules. Only the ratio of partition functions enter into these equilibrium constants and this makes it necessary to consider only these simple ratios, which are given for a chemical compound as

$$\frac{Q'_2}{Q'_1} = \frac{\sigma_1}{\sigma_2} \left(\frac{M_2}{M_1}\right)^{3/2} \frac{\sum \exp\left(-\frac{E_2}{kT}\right)}{\sum \exp\left(-\frac{E_1}{kT}\right)} \quad (34)$$

Where  $\sigma_1$ , and  $\sigma_2$  are the symmetry numbers of the two molecules,  $M_1$  and  $M_2$  are their molecular weights,  $E_1$  and  $E_2$  are particular energy states of the molecules, and the summations are to be taken over all such energy states.

The stable isotope fractionation factor between two compounds A and B is given by

$$\alpha_{A-B} = \frac{R_A}{R_B} = \frac{1000 + \delta_A}{1000 + \delta_B} \quad (35)$$

Or

$$10^3 \ln \alpha_{A-B} \cong \delta_A - \delta_B \quad (36)$$

where R's are isotope ratios of the element of interest in the respective compounds. The  $\delta$ -value of a sample A is defined as  $\delta = (R_A/R_{ST} - 1) \times 1000$ , where  $R_{ST}$  is the isotope ratio of the standard. The equilibrium constant of isotopic exchange reaction is directly related with the coefficient of fractionation  $\alpha$ . The values of  $\alpha$  are determined experimentally (Longinelli and Craig, 1967; Lloyd, 1968; Mizutani and Rafter, 1969) and theoretically (Urey, 1947; Zeebe, 2010). Recently, Zeebe (2010) presented a very systematic study on the determination and calculation of  $\alpha_{SO_4^{2-}-H_2O}$  and  $\alpha_{HSO_4^{2-}-H_2O}$  and proposed the following equations

$$10^3 \ln \alpha_{HSO_4^{2-}-H_2O} = 2.99 \frac{10^6}{T^2} - 4.95 \quad (37)$$

$$10^3 \ln \alpha_{SO_4^{2-}-H_2O} = 2.68 \frac{10^6}{T^2} - 7.35 \quad (38)$$

Initially, the equation 38 was used as isotope geothermometer; however, it is valid only at low pH of geothermal reservoir fluid (Zeebe (2010)).

Secondly, there are generally vapor and liquid in the geothermal reservoir. So, we consider the algorithm similar to the silica geothermometry to calculate the geothermal reservoir temperature and vapor fraction. Let the temperature and vapor fraction in the geothermal reservoir are  $T_{res}$  and  $y_{res}$ . The total discharge isotopic composition is written as

$$\delta^{18}O_{TD} = y_{res} \times \delta^{18}O_{vap,res} + (1 - y_{res}) \times \delta^{18}O_{liq,res} \quad (39)$$

The isotopic fractionation of oxygen-18 between the liquid and vapor phases in the reservoir as

$$10^3 \ln \alpha_{liq-vap} \cong \delta^{18}O_{liq,res} - \delta^{18}O_{vap,res} \quad (40)$$

Similarly, the isotopic fractionation of oxygen-18 between the dissolved sulfate and liquid phase in the reservoir as

$$10^3 \ln \alpha_{SO_4^{2-}-H_2O} \cong \delta^{18}O_{SO_4^{2-}} - \delta^{18}O_{liq,res} \quad (41)$$

These equations are used to calculate the  $T_{res}$ ,  $y_{res}$  and  $\delta^{18}O_{liq,res}$  (or  $\delta^{18}O_{vap,res}$ ). One more point to be emphasized is the analytical uncertainty in the measurement of  $\delta^{18}O_{H_2O}$  and  $\delta^{18}O_{SO_4^{2-}}$  are  $\pm 0.1$  and  $\pm 0.2 \text{‰}$ , respectively. This causes an uncertainty in the estimate of geothermal reservoir temperature from equations 39 and 42 of  $\pm 25^\circ\text{C}$  at  $T_{res}=250^\circ\text{C}$ .

#### 4. CASE STUDY: LOS AZUFRES

The cation-exchange and gas geothermometers limitations are illustrated above; therefore, this work presents only the applications of silica (quartz) and stable isotope ( $\delta^{18}O$  in  $SO_4^{2-}-H_2O$ ) in the determination of geothermal reservoir fluid characteristics. Table 2 presents the chemical analytical data of wells from Los Azufres geothermal field taken from Arellano et al. (2005) and Monteagudo (1989). Firstly, the separation pressure (PSep) from the separation temperature (TSep) is calculated using the SteamTables (Verma, 2003b). For example, the separation temperature of well 5 is  $180^\circ\text{C}$ . Using the SteamTables, the separation pressure is calculated as 1.003 MPa. The analytical uncertainty (error) is not reported in the analytical data of geothermal system. Verma et al. (2012) conducted an inter-laboratory comparison of silica analysis in water samples. They found that the analytical uncertainty in the silica analysis is more than 10%. Similarly, the uncertainty in the measurement of enthalpy is considered as 2%.

Verma (2012a) presented the calculation of geothermal reservoir temperature and vapor fraction in Excel. First, the total discharge silica concentration (SiO2TD) and its uncertainty (SiO2TDErr) are calculated. In the case of well 5, the input parameters are the number of separators ( $n_{Sep}=2$ ), separation pressures ( $PSep(1)=0.1$  and  $PSep(2)=1.003$  MPa), total discharge enthalpy ( $H_r=2224 \text{ kJ/kg}$ ), silica concentration in the water sample ( $SiO_2msd=991 \text{ ppm}$ ) and its uncertainty ( $SiO_2msdErr=99.1 \text{ ppm}$ ). Thus the total discharge concentration is  $230.5 \pm 23.1 \text{ ppm}$ . The propagation of uncertainty for the total discharge concentration is linear; therefore, the uncertainty in SiOTD is also 10%.

The geothermal reservoir temperature and vapor fraction and their uncertainties are calculated using the Excel function GeoRes. In the case of well 5, the input parameters are  $H_r=2224 \text{ kJ/kg}$ ,  $HrErr=2\% = 44.48 \text{ kJ/kg}$ ,  $SiO_2TD=231 \text{ ppm}$ ,  $SiO_2TDErr=23 \text{ ppm}$ , and  $GeoEQ=5$  (i.e. Quadratic of  $1/T$  and  $P$  with exact function constraints). Thus the calculated reservoir temperature and vapor fraction are  $T_{Res}=292 \pm 22^\circ\text{C}$  and  $y_{Res}=0.63 \pm 0.03$ . The present algorithm is based on the conservation of enthalpy; therefore, the enthalpy of the liquid and vapor at the reservoir temperature is the same as the total discharge enthalpy, i.e. no vapor loss or vapor gain between the deep fluid and the fluid reaching the surface was assumed.

Figure 7 shows the comparison of temperature and reservoir enthalpy, calculated from quartz geothermometry using the present algorithm (i.e. conservation of enthalpy) and the algorithm used in literature (i.e. liquid only in the reservoir). It can be observed in Figure 7(a) that the geothermal reservoir temperature of all the wells is significantly higher for the present algorithm than that used in the literature except for wells 22 and 26.

Figure 7(b) shows a relation between the measured and calculated enthalpies using the both the algorithms. The calculated enthalpies for well 26 are close since the vapor fraction ( $y_{Res}=0.13$ ) is low. As the vapor fraction increases the difference between the calculated enthalpies increases. The present algorithm is based on the conservation of enthalpy; therefore the measured and calculated enthalpies are same. If we consider the liquid only in the reservoir, there will be substantially low enthalpy in the reservoir. The energy loss is not feasible; therefore the present algorithm is an improved in the quartz geothermometry.

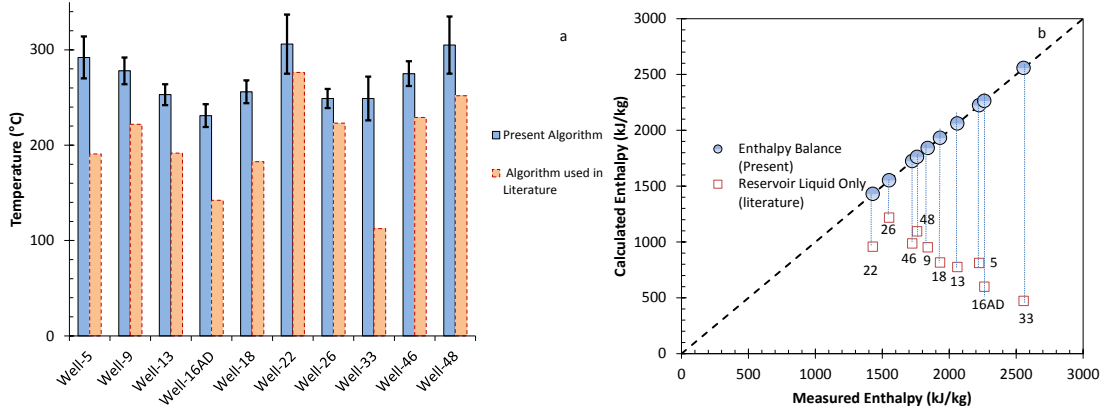


**Figure 7: Comparison of (a) reservoir temperature and (b) reservoir enthalpy for Los Azufres geothermal field, calculated by the quartz geothermometry using the present algorithm based on the conservation of enthalpy and the earlier algorithm considering only liquid in the reservoir. The data are slightly different from Verma (2012a) as the quadratic of  $1/T$  and  $P$  polynomial with exact function constraints is used for the quartz solubility.**

The enthalpy-pressure diagram for water is constructed in Excel using the SteamTables class (Verma, 2003b). The separation boundary between the liquid and vapor phases is formed by the critical isochor and the two phase region (Figure 8). The conditions of the geothermal reservoir fluids for all the wells are in the two phase region and between the isotherms at 200 and  $310^\circ\text{C}$ . Therefore, the geochemistry of Los Azufres provides the similar evidences as obtained by the well simulator (Arellano et al., 2005).

Verma et al. (2013) presented a comparative study of geochemical modeling of geothermal system using GeoSys.Chem and WATCH and concluded that both the programs provide similar results.

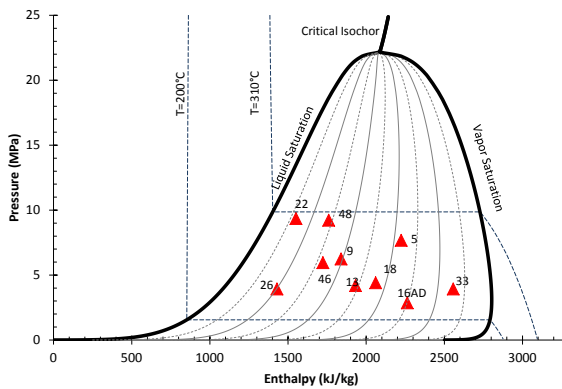


Figure 8: Enthalpy versus pressure diagram. It shows the characteristics of Los Azufres geothermal reservoir (after Arellano et al., 2005 and Verma, 2012b).

Table 3 presents the isotopic analytical data of wells from Los Azufres geothermal field taken from Monteagudo (1989). The reservoir enthalpy is considered from Arellano et al. (2005) as the objective of this chapter is to illustrate the calculation procedure only. As mentioned above the uncertainty in the reservoir temperature is at least  $\pm 25^\circ$ . We are working to write the computer program to propagate the uncertainty of all the analytical parameters.

**Table 2: Geothermal reservoir temperature and vapor fraction of Los Azufres geothermal reservoir, calculated from quartz geothermometry (data from Arellano et al., 2005) and isotope geothermometry (data from Monteagudo, 1989)**

Well	H <sub>r</sub> (kJ/kg)	T <sub>Sep</sub> (°C)	P <sub>atm</sub> (MPa)	P <sub>Sep</sub> (MPa)	SiO <sub>2</sub> (ppm)	SiO <sub>2,TD</sub> (ppm)	T <sub>SiO2</sub> (°C)	Vapor Fraction	Stable Isotope Geothermometer			
									δ <sup>18</sup> O <sub>TD</sub> (‰)	δ <sup>18</sup> O <sub>SO4</sub> (‰)	T <sub>SO4-H2O</sub> (°C)	Vapor Fraction
5	2224	180.0	0.1	1.003	991	231(23)	292(22)	0.63(3)	-3.72	2.51	202	0.71
9	1840	150.5	0.1	0.483	887	344(34)	278(14)	0.39(2)	-2.31	2.12	225	0.48
13	1932	170.0	0.1	0.792	661	234(23)	253(11)	0.49(2)	-2.39	2.20	224	0.53
16-AD	2263	172.0	0.1	0.831	509	109(11)	231(12)	0.70(2)	-3.37	2.64	206	0.72
18	2061	135.0	0.1	0.313	715	206(21)	256(12)	0.56(2)	-3.37	2.83	200	0.62
22	1551	190.5	0.1	1.269	1123	580(58)	306(31)	0.13(2)				
26	1430	177.0	0.1	0.935	617	349(35)	249(10)	0.20(2)				
33	2557	187.0	0.1	1.175	660	62(6)	249(23)	0.85(3)				
46	1724	160.5	0.1	0.626	850	374(37)	275(13)	0.33(2)	-3.07	3.11	193	0.46
48	1761	151.0	0.1	0.489	1124	474±47	305(30)	0.28(3)				

## 5. CONCLUSIONS

The quartz solubility geothermometry is an accurate and efficient approach to estimate the deep geothermal reservoir temperature and vapor fraction with multivariate analytical uncertainty propagation. The calculation of temperature and vapor fraction in the geothermal reservoir of Los Azufres geothermal system is illustrated with considering the analytical uncertainty of enthalpy (2%) and SiO<sub>2</sub> concentration (10%). The average uncertainty in the calculated reservoir temperature is  $\pm 20^{\circ}\text{C}$ .

The stable isotope geothermometry i.e. the fractionation of oxygen-18 in the dissolved sulfate and liquid water in the geothermal reservoir provides much lower temperatures, but there is relatively higher uncertainty at least  $\pm 25^\circ\text{C}$ . There are two possibilities: residence time of geothermal reservoir fluid is less to achieve the isotopic equilibrium or the equation 39 is incorrect.

The average uncertainty in the calculated reservoir temperature is  $\pm 20^\circ\text{C}$ , which is relatively high to understand reservoir processes during the exploitation of the geothermal reservoir. Thus the geochemical analysis of geothermal water is first improvement that must be made to obtain a better understanding of the characteristics of geothermal systems with fluid geochemistry. The algorithm of quartz geothermometry with considering only liquid phase in the geothermal reservoir is conceptually incorrect due to lacking of energy (enthalpy) balance. However, both the algorithms provide same results for the wells, which are fed from a single phase liquid reservoirs.

The Los Azufres geothermal reservoir temperature is 200–310°C and dominating process in the upper part of the reservoir is the evaporation and partial condensation.

**Acknowledgements.** This work was supported by the grant “FONDO SECTORIAL CONACYT-SENER SUSTENTABILIDAD ENERGÉTICA IIE-CEMIE-GEO-P14”

## REFERENCES

Arellano, V.M., Barragan, R.M., and Torres, M.A.: Thermodynamic evolution of the Los Azufres, Mexico, geothermal reservoir from 1982 to 2002, *Geothermics*, **34**, (2005), 592–616.

Arnórsson, S.: Chemical equilibria in Icelandic geothermal systems- implications for chemical geothermometry investigations, *Geothermics*, **12**, (1983), 119-128.

Arnórsson, S.: The quartz and Na/K geothermometers. I. new thermodynamic calibration. *Proceedings, World Geothermal Congress, Japan* (2000).

Fournier, R.O.: Chemical geothermometers and mixing models for geothermal systems, *Geothermics*, **5**, (1977a), 41-50.

Fournier, R.O.: The Solubility of amorphous silica in water at high temperature and pressure, *American Mineralogist*, **62**, (1977b), 1052-1056.

Fournier, R.O.: Lectures on geochemical interpretation of hydrothermal waters, *UNU Geothermal Training Programme, Iceland*, (1989).

Fournier, R.O., and Potter, R.W.: A revised and extended silica (quartz) geothermometer, *Geothermal Resources Council Bulletin*, **11**, (1982), 3-12.

Fournier, R.O., and Truesdell, A.H.: An empirical Na-K-Ca geothermometer for natural waters, *Geochimica et Cosmochimica Acta*, **37**, (1973), 1255-1275.

Giggenbach, W.F.: Geothermal gas equilibria, *Geochimica et Cosmochimica Acta*, **44**, (1980), 2021-2032.

Giggenbach, W.F.: Geothermal solute equilibria. Derivation of Na-K-Mg-Ca geoindicators, *Geochimica et Cosmochimica Acta*, **52**, (1988), 2749-2765.

Giggenbach, W.F., Tedesco, D., Sulistiyo, Y., Caprai, A., Cioni, R., Favara, R., Fisher, T.P., Hirabayashi, J.-I., Korzhinsky, M., Martini, M., Menyailov, I., and Shinohara, H.: Evaluation of results from the fourth and fifth IAVCEI field workshop on volcanic gases, Vulcano Island, Italy and Java, Indonesia, *Journal of Volcanology and Geothermal Research*, **108**, (2001), 157–172.

Gunnarsson, I., and Arnórsson, S.: Amorphous silica solubility and the thermodynamic properties of  $H_4SiO_4$  in the range of 0° to 350°C at  $P_{sat}$ , *Geochimica et Cosmochimica Acta*, **64**, (2000), 2295-2307.

Henley, R.W., Truesdell, A.H., Barton, P.B., and Whitney, J.A.: Fluid-Mineral Equilibria in Hydrothermal Systems, *Society of Economic Geologists, El Paso*, (1984).

Lloyd, R.M.: Oxygen isotope behavior in the sulfate–water system, *Journal of Geophysics Research*, **73**, (1968), 6099–6110.

Longinelli, A., and Craig, H.: Oxygen-18 variations in sulfate ions and sea water and saline lakes, *Science*, **156**, (1967), 56–59.

Mizutani, Y., Rafter, T.A.: Oxygen isotopic composition of sulphates—Part 3. Oxygen isotopic fractionation in the bisulphate ion–water system, *New Zealand Journal of Science*, **12**, (1969), 54–59.

Monteagudo, A.: Mediciones de temperaturas de yacimiento de campo geotérmico de Los Azufres con geotermómetro de isótopos ( $\delta^{18}O$  de agua y sulfato), *Thesis, Universidad Nacional Autónoma de México, D.F.* (1989).

Nieva, D., and Nieva, R.: Developments in geothermal energy in Mexico, part 12- A cationic composition goethermometer for prospection of geothermal resources, *Heat Recovery Systems and CHP*, **7**, (1987), 243-258.

Stumm, W., and Morgan, J.J.: Aquatic chemistry: an introduction emphasizing chemical equilibria in natural waters, 2<sup>nd</sup> ed., Wiley, New York, (1981).

Tonani, F.: Some remarks on the application of geochemical techniques in geothermal exploration, *Proceedings, Adv. Eur. Geoth. Res. Second Symp., Strasbourg*, (1980).

Truesdell, A.H.: Summary on section III geochemical techniques in exploration. *Proceedings, Second United Nations Symposium on the Development and Use of Geothermal Resources, San Francisco*, (1976).

Urey, H.C.: The thermodynamic properties of isotopic substances, *J. Chem. Soc.*, (1947), 562-581.

Verma, M.P.: Chemical thermodynamics of silica: a critique on its goethermometer, *Geothermics*, **29**, (2000), 323-346.

Verma, M.P.: Geochemical techniques in geothermal development, In: Chandrasekharan, D., Bundschuh, J. (Eds.), *Geothermal Energy Resources for Developing Countries*, The Swets & Zeitlinger Publishers, Netherlands, (2002a).

Verma, M.P.: A numerical simulation of  $H_2O$ - $CO_2$  heating in a geothermal reservoir, *Proceedings, Twenty-Seventh Workshop on Geothermal Reservoir Engineering, Stanford University, California*, (2002b).

Verma, M.P.: QrtzGeotherm: a computer program for the quartz solubility geothermometer in moderately saline brines up to 370°C, *Geothermal Research Council Transaction*, (2003a), 341-345.

Verma M.P.: Steam tables for pure water as an ActiveX component in Visual Basic 6.0, *Computer & Geoscience*, **29**, 1155-1163 (2003b)

Verma, M.P.: Thermodynamics, equations of state and experimental data: a review, *Journal of Engineering and Applied Sciences*, **1**, (2006), 35-43.

Verma, M.P.: QrtzGeotherm: an ActiveX component for the quartz solubility geothermometer, *Computer & Geoscience*, **34**, (2008), 1918-1925.

Verma, M.P.: QrtzGeotherm: a revised algorithm for quartz solubility geothermometer to estimate geothermal reservoir temperature and vapor fraction with multivariate analytical uncertainty propagation, *Computer & Geoscience*, **48**, (2012a), 316-322.

Verma, M.P.: GeoSys.Chem: Estimate of reservoir fluid characteristics as first step in geochemical modeling of geothermal systems, *Computer & Geoscience*, **49**, (2012b), 29-37.

Verma, M.P.: Steam Transport simulation in a geothermal pipeline network constrained by internally consistent thermodynamic properties of water, *Revista Mexicana de Ciencias Geológicas*, **30**, (2013), 210-221

Verma, M.P., and Betzler, K.: Chemical geothermometry in evaluation of geothermal reservoir characteristics: a thermodynamic point of view. *Acta INAGEQ*, **19**, (2013), 155-161.

Verma, M.P.: Geothermometry in Exploration and Exploitation of Geothermal System, In J.N. Govil (ed.), *Geothermal and Ocean Energy*, vol. 7, Publishers Studium Press LLC, USA, (2014).

Verma, M.P., Izquierdo, G., Urbino, G.A., Gangloff, S., Garcia, R., Aparicio, A., Conte, T., Armienta, M.A., Sanchez, M., Gabriel, J.R.P., Fajanel, I.D., Renderos, R., Acha, C.B.A., Prasetio, R., Grajales, I.C., Delgado, L.R., Opondo, K., Esparza, R.Z., Panama, L.A., Salazar, R.T., Lim, P.G., Javino, F.: Inter-laboratory comparison of SiO<sub>2</sub> analysis for geothermal water chemistry, *Geothermics*, **44**, (2012), 33-42.

Verma, S.P.: Optimisation of the exploration and evaluation of geothermal resources, In: Chandrasekharam, D., Bundschuh, J. (Eds.), *Geothermal Energy Resources for Developing Countries*, The Swets & Zeitlinger Publishers, Netherlands, (2002).

Verma, S.P., and Santoyo, E.: New improved equation for Na/K, Na/Li and SiO<sub>2</sub> geothermometer by outlier detection and rejection, *Journal of Volcanology and Geothermal Research*, **79**, (1997), 9-23.

White, D.E., and Brannock, W.W., and Murata, K.J.: Silica in hot-spring waters, *Geochimica et Cosmochimica Acta*, **10**, (1956) 27-59.

Zeebe, R.E.: A new value for the stable oxygen isotope fractionation between dissolved sulfate ion and water, *Geochimica et Cosmochimica Acta*, **74**, (2010), 818-828.